^{70}Zn(p,t)^{68}Zn reaction at $E_p = 35$ MeV

M. Carchidi,* M. Burlein, H. T. Fortune, G. P. Gilfoyle,† R. Gilman,‡ J. Görres,§
P. Kutt, S. Saini,** and J. W. Sweet
Department of Physics, University of Pennsylvania, Philadelphia, Pennsylvania 19104

R. T. Kouzes and R. Sherr
Department of Physics, Princeton University, Princeton, New Jersey 08541
(Received 31 May 1988)

We have investigated the ^{70}Zn(p,t)^{68}Zn reaction using a beam energy of 35 MeV. Angular distributions were extracted for 18 levels up to 4.25 MeV excitation in ^{68}Zn. Distorted-wave Born-approximation calculations have been performed and compared to each angular distribution. Because the distorted-wave Born-approximation angular distributions to the lowest 2^+, 3^-, and 4^+ states in ^{68}Zn are found to be a poor representation of the data, we have also performed coupled-channels Born-approximation calculations for the ^{70}Zn(p,t) reaction leading to these states.

I. INTRODUCTION

The ^{68}Zn nucleus has been studied via many direct reactions. Available information and references are summarized in the latest compilation.[1] The ^{70}Zn(p,t)^{68}Zn reaction had been investigated earlier[2] using a 17.5-MeV proton beam, but poor resolution allowed extraction of data for only seven levels. In addition, the 0_2^+ level in ^{68}Zn at 1.656 MeV was not fully resolved from the ^{66}Zn ground state which is about 120-keV higher in Q value. Therefore, the $\sigma(0_2^+)/\sigma$(g.s.) ratio was not determined in that reference. This ratio is essential for performing a two-state coexistence model analysis for zinc similar to that done for the germanium isotopes.[3] We have measured this ratio accurately and have already analyzed[4] the ground and 0_2^+ states in even zinc isotopes within the framework of this two-state coexistence model. Herein, we report on all the data that were obtained in the ^{70}Zn(p,t)^{68}Zn reaction at a proton beam energy of 35 MeV.

Angular distributions have been extracted for 18 states up to 4.25-MeV excitation in ^{68}Zn and compared to standard distorted-wave Born-approximation (DWBA) calculations. In addition, we performed coupled-channels Born-approximation calculations (CCBA) for the ^{70}Zn(p,t) reaction leading to the lowest 2^+, 3^-, and 4^+ states in ^{68}Zn.

II. EXPERIMENTAL PROCEDURE

Data for the ^{70}Zn(p,t)^{68}Zn reaction were acquired with a 35-MeV proton beam from the Princeton cyclotron. The outgoing tritons were momentum analyzed through a QDDD spectrometer (with a 6° angular resolution) and detected using a 120-cm resistive division type[5] position-sensitive gas proportional counter. In this way, we were able to measure up to 4.25-MeV excitation in ^{68}Zn using only two momentum bites and still leave much overlap between the two bites. The gas counter was backed by a pilot M plastic scintillator and the electronics were set up to require a coincidence between the gas counter and scintillator. This coincidence requirement eliminated much of the background from other reactions, as the particle identifier of gas signal versus scintillator signal shows distinct particle groups. The above coincidence requirement allowed us to place an accurate software window around the triton group resulting in a typical triton spectrum shown in Fig. 1. The energy resolution is approximately 35 keV and the uncertainty in the measured *relative* cross section is about 10%. We used a 65 μg/cm^2, 85.03% enriched ^{70}Zn target which was floated onto a 35 μg/cm^2 ^{12}C backing. The ^{70}Zn target contained enough ^{68}Zn ($\approx$4.65%) to see the ground state and 2_1^+ state of ^{66}Zn. However, the good resolution of the spectrometer system allowed us to easily resolve these states in ^{66}Zn from the energy levels in ^{68}Zn. Specifically, we were able to easily resolve the ground state of ^{66}Zn

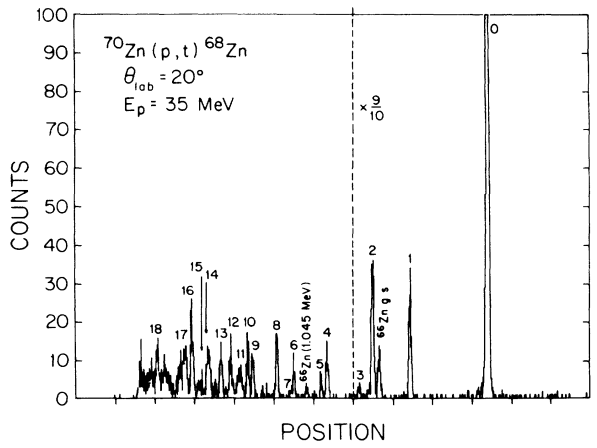

FIG. 1. Energy spectrum of the ^{70}Zn(p,t)^{68}Zn reaction at $E_p = 35$ MeV and $\theta_{lab} = 20°$. Also labeled are the ground and 2_1^+ states seen in ^{68}Zn(p,t)^{66}Zn.

 ©1988 The American Physical Society

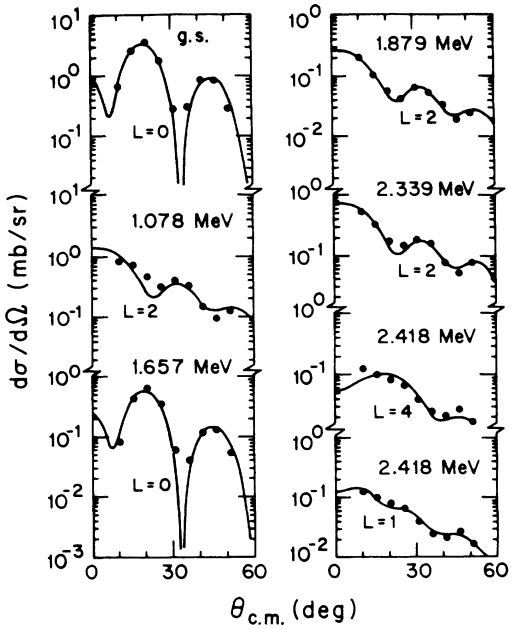

FIG. 2. Angular distributions and DWBA fits for states seen in ^{68}Zn from $E_x = 0.0$ to 2.418 MeV.

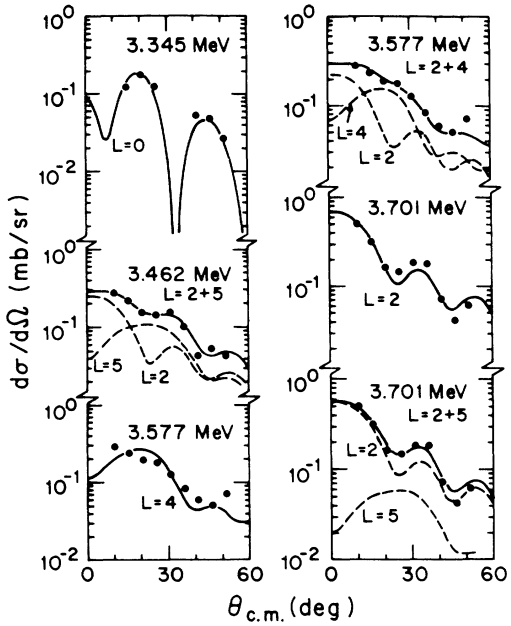

FIG. 4. Angular distributions and DWBA fits for states seen in ^{68}Zn from $E_x = 3.345$ to 3.701 MeV.

from the 1.656-MeV state in ^{68}Zn as shown in Fig. 1.

III. RESULTS AND ANALYSIS

Measurable cross sections were observed for 18 levels up to 4.25-MeV excitation in ^{68}Zn. Excitation energies were obtained using the ground state and the first three excited states in ^{68}Zn as calibrates in the first momentum bite and the second to seventh excited states in ^{68}Zn as the calibrates in the second momentum bite. This procedure allowed identification of 23 excitation energies for levels existing in ^{68}Zn. These energies are constant with center of mass angle which is an indication of a good calibration. The largest deviations from constancy occurred near the edges of the detector where nonlinear effects become important. In order to avoid these edge effects of the detector, we use the results of the first momentum bite to study the angular distributions of the ground states in ^{68}Zn and ^{66}Zn and the first three excited states in ^{68}Zn while we use the results of the second momentum bite to study the angular distributions of the remaining

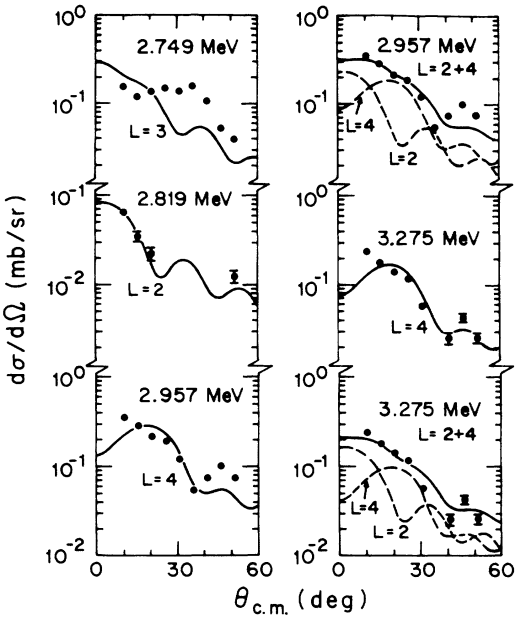

FIG. 3. Angular distributions and DWBA fits for states seen in ^{68}Zn from $E_x = 2.749$ to 3.275 MeV.

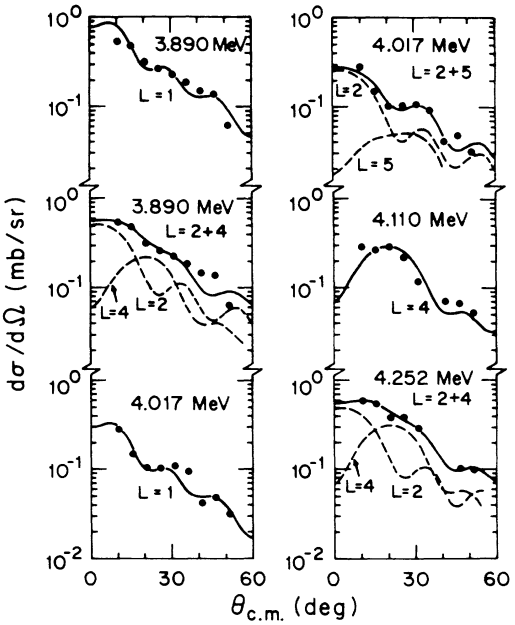

FIG. 5. Angular distributions and DWBA fits for states seen in ^{68}Zn from $E_x = 3.890$ to 4.252 MeV.

TABLE I. Optical-model parameters[a] used in the DWBA analysis.

	V (MeV)	r_0 (fm)	a (fm)	W (MeV)	$W'=4W_D$ (MeV)	r_0' (fm)	a' (fm)	r_c (fm)
p	50.5	1.17	0.65		60.0	1.25	0.47	1.30
t	168.0	1.20	0.65	13.5		1.60	0.87	1.30

[a]The optical-model parameters for both the incident and exit channels are from the works of Perey (Ref. 7) and Hardekopf (Ref. 8), respectively, with some modifications. They are identical to those used in earlier ^{76}Ge$(t,p)^{78}$Ge work (Ref. 9) with a change in the radius of the real part of the proton optical-model potential from 1.25 to 1.17 fm.

states seen in the reaction.

Angular distributions for lab angles from 10° to 50° in steps of 5° were extracted for all levels observed at four or more angles, and compared with the results of DWBA calculations using the code DWUCK4.[6] The optical-model parameters for both the incident and exit channels are from the works of Refs. 7 and 8, respectively, with some modifications. These are given in Table I and they are identical to those used in earlier ^{76}Ge$(t,p)^{78}$Ge work[9] with a change in the radius of the real part of the proton optical-model potential from 1.25 to 1.17 fm. This *same* radius value was used by Rosier *et al.*[10] in the study of Ge(p,p') at 22 MeV although the real well depth of the proton was a little larger. Figures 2–5 display the angular distributions for the states of ^{68}Zn along with the calculated fits. In all the calculations we assumed pure shell-model configurations for the transferred neutron pair: $(2p_{1/2})_0^2$ for $L=0$; $(1g_{9/2})_L^2$ for $L=2$, 4, and 6; $(1g_{9/2}1f_{7/2})$ for $L=1$; $(1g_{9/2}1f_{5/2})$ for $L=3$; and $(1g_{9/2}2p_{1/2})$ for $L=5$. Various combinations of these configurations produced results that differed from the pure calculations in magnitude but only very slightly in shape. Table II summarizes the excitation energies, L and J^π values, and maximum measured cross sections for each level seen in ^{68}Zn and ^{66}Zn. Also presented in Table II is a summary of earlier ^{66}Zn$(t,p)^{68}$Zn work.[11]

TABLE II. Summary of levels seen in ^{68}Zn.

	Present work				^{66}Zn$(t,p)^{68}$Zn[b]			Compilation[c]	
	E_x[a] (MeV)	σ_{max} (μb/sr)	L	J^π	E_x (MeV)	J^π	σ_{max} (μb/sr)	E_x (MeV)	J^π
0	0.0	1274	0	0^+	0.0	0^+	4800	0.0	0^+
1	1.078	298	2	2^+	1.075	2^+	119	1.077	2^+
	^{66}Zn(g.s.)	1455	0	0^+					
2	1.657	231	0	0^+	1.656	0^+	59	1.656	0^+
3	1.879	74	2	2^+	1.881		18	1.883	2^+
4	2.339	190	2	2^+	2.334	2^+	163	2.338	2^+
								2.370	
5	2.418	45	4	4^+	2.416		19	2.417	$(4)^+$
			or 1	or 1^-					
	^{66}Zn(2_1^+)	525	2	2^+					
			or 1	or 1^-					
								2.510	
6	2.749	57	3[d]	3^-	2.747	3^-	79	2.751	3^-
7	2.819	23	2	2^+	2.821	2^+	27	2.822	2^+
8	2.957	127	4	4^+	2.955	4^+	33	2.956	(4^+)
			4+(2)						
								2.960	
								3.009	
								3.080	
					3.100	0^+	41	3.102	0^+
								3.154	
					3.157	0^+	530	3.157	0^+
								3.160	
								3.164	
								3.184	$(1,2^+)$
								3.186	$1^+,2^+$
9	3.275	87	4 + (2)	4^+	3.278	4^+	15	3.282	4^+
								3.287	$(2)^+$
10	3.345	66	(0)	(0^+)				3.346	
								3.385	
								3.401	
								3.425	

TABLE II. (*Continued*).

	Present work				^{66}Zn(t,p)^{68}Zn[b]			Compilation[c]	
	E_x[a] (MeV)	σ_{max} (μb/sr)	L	J^π	E_x (MeV)	J^π	σ_{max} (μb/sr)	E_x (MeV)	J^π
					3.427	2^+	27	3.429	2^+
11	3.462	99	2 + 5		3.451	5^-	29	3.458	5^-
					3.492		15	3.490	+
								3.496	
12	3.577	103	4 + (2)	4^+	3.583	(4^+)	9	3.587	(4^+)
								3.610	(6)
					3.620	3^-	28	3.620	3^-
								3.624	
								3.630	
								3.665	$(1,2)^+$
					3.682	(5^-)	14	3.688	
13	3.701	183	2	2^+					
					3.712	4^+	18	3.710	
						0^+	32		
								3.718	(1)
								3.720	3^-
								3.726	
								3.732	+
								3.773	
								3.776	$(1,2^+)$
					3.806	(3^-)		3.806	3^-
								3.815	
					3.841	4^+	34	3.849	4^+
14	3.890	192	4 + (2) or 1	4^+	3.886	4^+	34	3.896	4^+
					3.927		59	3.911	
15	4.017	102	2 or 1	2^+ or 1^-	4.049	(2^+)	48		
16	4.110	107	4						
					4.145	0^+	43		
17	4.252	215	2 + 4		4.268		118		
								4.339	$(1)^-$
								4.466	1
								4.503	(1)

[a]Energies were calculated as discussed in Sec. III of the text.
[b]Taken from Ref. 11.
[c]Taken from Ref. 1.
[d]Based on the CCBA calculations in Sec. V B.

IV. DISCUSSION OF LEVELS IN ^{68}Zn

The ground state of ^{70}Zn, of course, has $J^\pi=0^+$, so assuming that the two transferred neutrons in (p,t) couple to spin zero, the spin and parity of the final state in ^{68}Zn is determined by the transferred angular momentum and hence by the shape of the angular distribution. The ground-state angular distribution (Fig. 2) possesses a characteristic $L=0$ shape, as expected for a $J^\pi=0^+$ state.

It is well known that the spin and parity of the 1.078-MeV state is 2^+, but the $L=2$ DWBA curve (Fig. 2) does not reproduce its angular distribution. Angular distributions of other known 2^+ states (to be discussed later) are reproduced quite well by DWBA. The angular distribution of the 2_1^+ state has its forward-angle slope less steep than that of other 2^+ angular distributions. This observation is not new and was observed in (p,t) on the selenium isotopes,[12] although it is not as prominent in zinc as in selenium. The inability of DWBA to reproduce the angular distribution of this state may suggest a two-step direct process, a discussion of which is given in Sec. V A of this report.

The good fit to an $L=0$ shape displayed in Fig. 2 for the angular distribution of the 1.657-MeV state makes it the first excited 0^+ state seen in (p,t) and its strength (at the 20° point) is about 18% of that for the ground state. As mentioned, the knowledge of $\sigma(0_2^+)/\sigma$ (g.s.) is essential in applying a two-state model analysis for zinc[4] as was done for germanium.[3]

Angular distributions for both the 1.879 and 2.339-MeV states are well fitted by $L=2$ shapes, as seen in Fig. 2. There is no hint of the difficulty encountered for the 1.078-MeV state. A state at 2.370 MeV in Ref. 1, with no

J^π information, is not apparent in our spectra (Fig. 1).

The recent compilation[1] assigns the 2.418-MeV level positive parity and a tentative $J=4$. Figure 2 shows that an $L=4$ curve does a reasonable job fitting the angular distribution, although the $L=4$ curve is a bit low at the 10° point. We shall see that this effect is present for all our $L=4$ angular distributions. Changing the configuration of the transferred neutron pair does not improve the fit at the 10° point. If we attempt to fit the angular distribution of this 2.418-MeV level with an $L=1$ curve, we obtain a much better fit. Of course, an $L=1$ fit would give a J^π of 1^- for this level and it is rare for a nucleus in this mass region to have a 1^- state below its first 3^- state. In any case, the angular distribution for this state cannot distinguish between $L=1$ and $L=4$ DWBA curves. However, if the parity in Ref. 1 is definite, we can make a 4^+ assignment. In an attempt to improve the fit at the 10° point, we have performed CCBA calculations (Sec. V C) to this state.

The compilation lists a state (with no J^π assignment) at 2.510 MeV. If present in our work, this state could perhaps be the extremely weak peak in Fig. 1 between level 5 and the impurity peak from ^{68}Zn(p,t) at 1.045 MeV excitation in ^{66}Zn.

The state at 2.751 MeV is the first 3^- state in ^{68}Zn reported in the compilation.[1] It was observed in inelastic electron scattering,[13–15] and in ^{66}Zn$(t,p)^{68}$Zn with a *very firm* $L=3$ angular distribution. We observe a state at 2.749 MeV, but as noted in Fig. 3, an $L=3$ DWBA curve *shows no* reasonable resemblance to this angular distribution. The inability of DWBA to reproduce angular distributions characterized by $L=3$ states is evident in other (p,t) reactions in this mass region. Specifically, in ^{66}Zn$(p,t)^{64}$Zn at 35 MeV,[16] the 3^- state at 3.02 MeV is poorly fitted by DWBA, a 3^- state at 3.72 MeV is not observed, whereas a 3^- state at 4.4 MeV is well fitted. We shall show in Sec. V B that two-step CCBA calculations to this state reproduce the observed ^{70}Zn$(p,t)^{68}$Zn(3_1^-) angular distribution very well.

The weak state we observe at 2.819 MeV (Fig. 3) is probably the 2^+ state in the compilation and observed in ^{66}Zn(t,p). Because of this correspondence, we compare the data to an $L=2$ curve. There is no disagreement, but several of our data points are missing for this state because it is too weak to extract at several angles.

Our level 8, at 2.957 MeV, undoubtedly contains contributions from two states—at 2.956 and 2.960 MeV in Ref. 1. The former has a tentative (4^+) assignment and was assigned 4^+ in (t,p). The latter level is not listed in the (t,p) work, but it would probably not have been resolved. An $L=4$ DWBA curve fits the data reasonably well, but there is perhaps some evidence of another L value—probably $L=2$.

The compilation lists nine states between 3.01 and 3.20 MeV, only two of which (0^+ levels at 3.100 and 3.157 MeV) were observed[11] in (t,p). None of these nine states are strong enough in ^{70}Zn(p,t) to allow extractions of angular distributions, although at least two weak peaks are apparent in Fig. 1 between levels 8 and 9.

In ^{66}Zn(t,p), a 4^+ level was observed at 3.278 MeV, probably to be identified with the 4^+ state at 3.282 MeV in the compilations—which also lists a $(2)^+$ state at 3.287 MeV. Our angular distribution (Fig. 3) for a state at 3.275 MeV is dominated by $L=4$, with an indication of some contribution from $L=2$.

The 3.345-MeV angular distribution (Fig. 4) appears to be of $L=0$ shape, although data are missing at several crucial angles. This state is probably to be identified with the level at 3.346 MeV in Ref. 1. This level was not observed in ^{66}Zn(t,p).

Our next "state" has a centroid of 3.462 MeV, but the peak corresponding to it in our spectrum (Fig. 1) is quite broad (80 keV). Hence, it undoubtedly contains contributions from more than one of the six levels listed in the compilation at 3.401, 3.425 (both with no J^π information); 3.429, 2^+; 3.458, 5^-; 3.490 ($\pi=+$); and 3.496 MeV (no J^π assignment). Of these six, three were observed in ^{66}Zn(t,p)—at $E_x=3.427$ MeV ($J^\pi=2^+$), 3.451 MeV ($J^\pi=5^-$), and 3.492 MeV (no J^π assignment). Our angular distribution (Fig. 4) is very nicely fitted by $L=2+5$, indicating that the present state is dominately a mixture of the 2^+ and 5^- states listed in the compilation and seen in ^{66}Zn(t,p).

The angular distribution of the state at 3.577 MeV (Fig. 4) is dominated by $L=4$, which is consistent with the tentative (4^+) assignment for a 3.587-MeV state in the compilation. However if a doublet exists, then addition of a small amount of $L=2$ improves the fit. Several states listed in the compilation at 3.610 MeV ($J=6$), 3.620 MeV ($J^\pi=3^-$), 3.624 MeV (no J^π assignment), 3.630 MeV (no J^π assignment), 3.665 MeV ($J^\pi=1^+$ or 2^+), and 3.688 MeV (no J^π assignment) are not seen in the present ^{70}Zn(p,t) reaction. Only two of these states (3.620 and 3.682 MeV) are reported in ^{66}Zn(t,p).

The angular distribution of the 3.701-MeV state is dominated by $L=2$ (Fig. 4) implying 2^+. However, the first minimum in that angular distribution is filled in as compared to the corresponding minimum of the DWBA $L=2$ calculation. This extra strength in the angular distribution can be attributed to the presence of the 5^- state seen in ^{66}Zn(t,p) about 19 keV lower in excitation as it is clear from Fig. 4 that a small admixture of $L=5$ greatly improves the fit of the data. Nevertheless, the evidence for $L=2$ is compelling and no 2^+ level is reported in this excitation energy region. We therefore place it between the states at 3.688 MeV and 3.710 MeV. Several states listed in the compilation at 3.718 MeV ($J=1$), 3.720 MeV ($J^\pi=3^-$), 3.726 MeV (no J^π assignment), 3.732 MeV ($\pi=+$), 3.773 MeV (no J^π assignment), 3.776 ($J^\pi=1$ or 2^+), 3.806 ($J^\pi=3^-$), 3.815 MeV (no J^π assignment), and 3.849 MeV ($J^\pi=4^+$) are not seen in the present ^{70}Zn(p,t) reaction. Only two of these states (3.806 and 3.841 MeV) are reported in ^{66}Zn(t,p).

The angular distribution for the 3.890-MeV level (Fig. 5) seems to contain at least two L values—$L=4+2$. Since the compilation and earlier (t,p) work report a 4^+ state at 3.886 MeV, we are probably seeing a doublet, one member having $J^\pi=4^+$, the other 2^+. However, a reasonable fit to the angular distribution is obtained with a pure $L=1$ curve. Again we see the difficulty of the angular distribution data to distinguish between $L=1$ and $L=2+4$. An energy level listed at 3.911 MeV in the

complilation and seen in earlier ^{66}Zn(t,p) work is not observed in the present ^{70}Zn(p,t) investigation.

The peak corresponding to our 4.017-MeV state is broader than our resolution—suggesting an unresolved doublet. A state at 4.049 MeV was assigned (2^+) in ^{66}Zn(t,p). The nearest known states are more than 100 keV away on either side. An $L=2$ curve (Fig. 5) fits our forward-angle data reasonably well. The first minimum, however, is filled in as with the 3.701-MeV state discussed earlier. A small addition of $L=5$ improves the fit substantially. On the other hand, a pure $L=1$ curve fits the shape of this angular distribution just as well. The presence of other L values is not compelling. Based on this work and earlier ^{66}Zn(t,p) results, however, the 4.017-MeV state probably has $J^\pi=2^+$. In Fig. 5 we see a reasonably firm $L=4$ shape for the angular distribution of the 4.110-MeV state, implying $J^\pi=4^+$. The angular distribution for the 4.252-MeV state (Fig. 5) is reproduced quite well by equal amounts of $L=2+4$ shapes suggesting a possible $(2^+,4^+)$ doublet. The peak is certainty wide enough (Fig. 1) to contain more than one state.

V. CCBA CALCULATIONS FOR THE LOWEST 2^+, 3^-, and 4^+ STATES IN ^{68}Zn

In this section we consider coupled-channels Born-approximation (CCBA) calculations for the cross sections in the ^{70}Zn(p,t) reaction leading to the lowest 2^+, 3^-, and 4^+ states in ^{68}Zn. We consider only these states since it is these states that are strongly coupled to the ground state via electromagnetic transitions. It is clear from the above discussions (Figs. 2 and 3) that the one-step direct DWBA calculations are not capable of accounting for the shapes of the angular distributions of the lowest 2^+, 3^-, and 4^+ levels seen in ^{70}Zn(p,t). We shall see below that a CCBA calculation is adequate for describing both the shapes and magnitudes of these angular distributions, but two or more routes are necessary.

A. The 2_1^+ state

We return now to the anomalous shape of the angular distribution of the lowest 2^+ state. In terms of peak cross section, this state is stronger than any other *excited* state, but only about 20% as strong as the ground state. It also is connected to the ground state by a large $E2$ matrix element, as is the 2_1^+ level in ^{70}Zn connected to its ground state. Thus, if inelastic two-step processes are to affect any state, the lowest 2^+ level is an excellent candidate.

We have performed coupled-channels calculations with the code CHUCK4.[6] As a foundation for these calculations we start with the ^{70}Zn(g.s.)$\rightarrow^{68}$Zn(g.s.) cross section and build upon this by coupling the elastic ^{70}Zn(g.s.) transition and inelastic ^{68,70}Zn(g.s.)$\rightarrow^{68,70}$Zn(2_1^+) transitions along with the ^{70}Zn$(2_1^+)\rightarrow^{68}$Zn(2_1^+) transition. These processes are all indicated schematically in Figs. 6 and 7. In these calculations, the spectroscopic strength for the

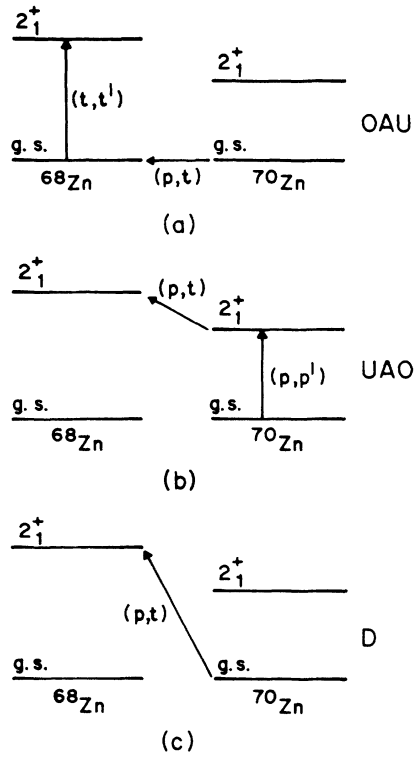

FIG. 6. Schematic representation of the three processes: (a) ^{70}Zn(g.s.)$\rightarrow^{68}$Zn(g.s.)$\rightarrow^{68}$Zn(2_1^+), denoted by OAU; (b) ^{70}Zn(g.s.)$\rightarrow^{70}$Zn$(2_1^+)\rightarrow^{68}$Zn(2_1^+), denoted by UAO; and (c) ^{70}Zn(g.s.)$\rightarrow^{68}$Zn(2_1^+), denoted by D.

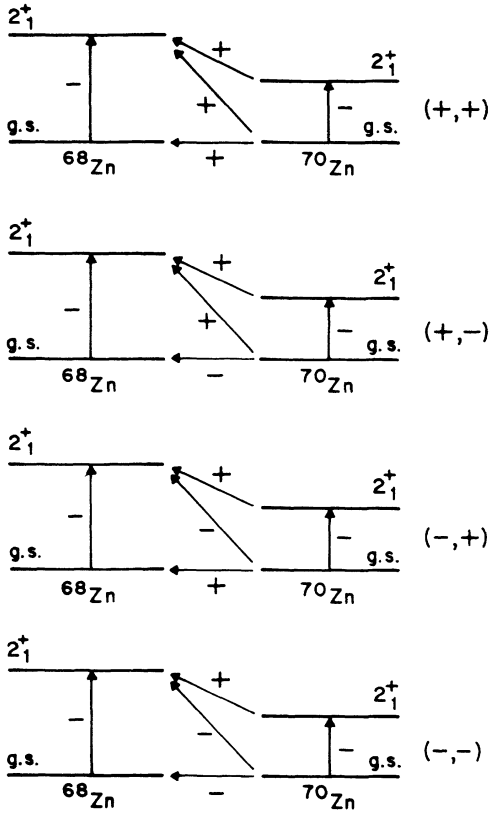

FIG. 7. Schematic representation of the four processes: $(+,+)$, $(+,-)$, $(-,+)$, and $(-,-)$.

^{70}Zn(g.s.)$\rightarrow$^{68}Zn(g.s.) process was chosen to reproduce the experimental ^{70}Zn(p,t)^{68}Zn(g.s.) cross section in both shape and magnitude. The spectroscopic strength for the ^{70}Zn(2_1^+)$\rightarrow$^{68}Zn(2_1^+) process was taken to be equal to the ground-state value, and containing only $L=0$. For the inelastic part of the transition, we take the values of β_2 from measurement. In ^{70}Zn(p,p') at 35.2 MeV,[17] β_2 is measured to have a magnitude of 0.19 and is "assigned" to be negative. We shall take $\beta_2=-0.19$ but we will consider calculations involving all possible sign combinations in the couplings so that knowledge of the sign of β_2 is not necessary. Data for ^{68}Zn(t,t') do not exist, but ^{68}Zn(p,p') gives[17] the magnitude of β_2 to be 0.19 with the same sign as that of the β_2 value in ^{70}Zn. Thus, with these values of β_2 and the ^{70}Zn(g.s.)$\rightarrow$^{68}Zn(g.s.) and ^{70}Zn(2_1^+)$\rightarrow$^{68}Zn(2_1^+) pickup normalizations referred to above, the magnitudes (although not the signs) of the two-step routes are fixed. We consider calculations involving the over-and-up (OAU) route, the up-and-over (UAO) route and the direct route (D) (displayed schematically in Fig. 6) along with various combinations of these which are displayed schematically in Fig. 7.

The direct calculation (D) is just DWBA and was discussed already in Sec. IV. The results of the coupled-channels Born-approximation calculations using the UAO and OAU routes are shown in Fig. 8 along with the angular distribution of the 1.078-MeV state in ^{68}Zn. In these single-route calculations, the sign of the spectroscopic amplitude connecting ^{70}Zn(g.s.) and ^{68}Zn(g.s.) in the OAU route and connecting ^{70}Zn(2_1^+) and ^{68}Zn(2_1^+) in the UAO route does not effect the final result. One sees that the shape of the UAO calculation fits the forward angles quite well, but the magnitude underestimates the data by a factor of 3.4. In addition, the second maximum in the data is not reproduced. The OAU calculation underestimates the data by a factor of 11 and does not have the necessary structure in the shape.

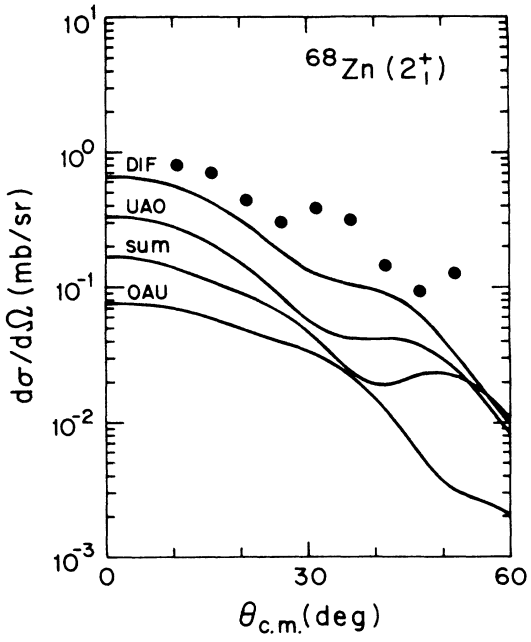

FIG. 8. CCBA calculations for processes UAO, OAU, |UAO + OAU|, and |UAO−OAU| along with the ^{70}Zn(p,t)^{68}Zn(2_1^+) angular distribution.

To improve the quality of the fit, we have also considered calculations which couple the OAU and UAO routes. These are also shown in Fig. 8. Here two possible calculations result depending on whether the signs of the spectroscopic amplitude connecting ^{70}Zn(g.s.) and ^{68}Zn(g.s.) in the OAU calculation and connecting ^{70}Zn(2_1^+) and ^{68}Zn(2_1^+) in the UAO calculation are the same or different. The general shapes of the two calculations are not very different, but the magnitude of the data is better reproduced when the signs between the spectroscopic amplitude connecting ^{70}Zn(g.s.) and ^{68}Zn(g.s.) in the OAU calculation and connecting ^{70}Zn(2_1^+) and ^{68}Zn(2_1^+) in the UAO calculation are different. In all of the CCBA calculations above, the forward angles of the data are better reproduced than in DWBA, but the second maximum is not. In fact, DWBA does a better job in reproducing the second maximum in the data. This suggests that one should consider a CCBA calculation which couples the UAO and OAU routes *along* with the direct (D) route. Of course, the problem here is that one does not know how much spectroscopic strength to include in the direct part of the calculation. In addition, there exist two possible calculations depending on the choice of sign for the one-step amplitude even if other signs have been determined. We take the spectroscopic amplitude of the ^{70}Zn(2_1^+)$\rightarrow$^{68}Zn(2_1^+) route to be positive and then vary the signs of the spectroscopic amplitude of the ^{70}Zn(g.s.)$\rightarrow$^{68}Zn(2_1^+) and the ^{70}Zn(g.s.) $\rightarrow$^{68}Zn(g.s.) routes labeling them as (+,+), (+,−), (−,+), and (−,−), respectively (see Fig. 7). To determine the spectroscopic strength for the ^{70}Zn(g.s.) $\rightarrow$^{68}Zn(2_1^+) route of each calculation, we at first choose that strength which reproduces the 1.078-MeV data in magnitude using only the ^{70}Zn(g.s.)$\rightarrow$^{68}Zn(2_1^+) component of the calculation. We then increase or decrease the ^{70}Zn(g.s.)$\rightarrow$^{68}Zn(2_1^+) one-step strength until a fit in magnitude is obtained for the two-step calculation. This process is performed for each of the four sign combinations (in Fig. 7). In all four possible sign combinations, the *magnitude* of the ^{70}Zn(p,t)^{68}Zn(1.078 MeV) angular distribution can be reproduced by a sufficient choice of strength in the ^{70}Zn(g.s.)$\rightarrow$^{68}Zn(2_1^+) route. On the other hand, the *shape* of this angular distribution (Fig. 9) is reproduced only by the (−,+) sign combination and allowing the ^{70}Zn(g.s.)$\rightarrow$^{68}Zn(2_1^+) strength to be 16% larger in magnitude than when using only the ^{70}Zn(g.s.)$\rightarrow$^{68}Zn(2_1^+) component of the calculation. We then fit both the shape and magnitude of the data very well. The other three possible sign combinations [i.e., (+,+), (+,−), and (−,−)] do reproduce the magnitude [with suitable choices for the ^{70}Zn(g.s.)$\rightarrow$^{68}Zn(2_1^+) strength], but they do not reproduce the shape of the angular distribution very well (Fig. 9). The best-fit CCBA calculation and the DWBA results are shown with the data in Fig. 10. One sees that the difference between the two calculations is significant, unlike earlier results found in the lighter-mass ^{40}Ar(p,t) reaction analysis.[18]

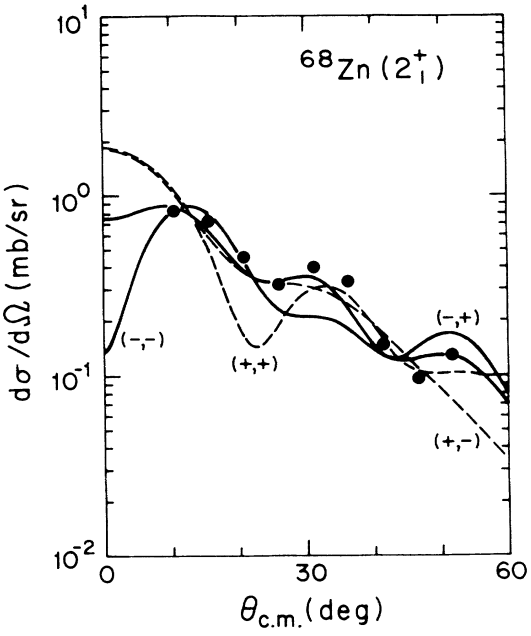

FIG. 9. Coupled-channels calculations including all the processes UAO, OAU, and D along with the ^{70}Zn(p,t)^{68}Zn(2_1^+) angular distribution. In all four curves, the strength of the ^{70}Zn(g.s.)→^{68}Zn(2_1^+) route has been varied to give the best-fit magnitude to the measured ^{70}Zn(p,t)^{68}Zn(2_1^+) cross section.

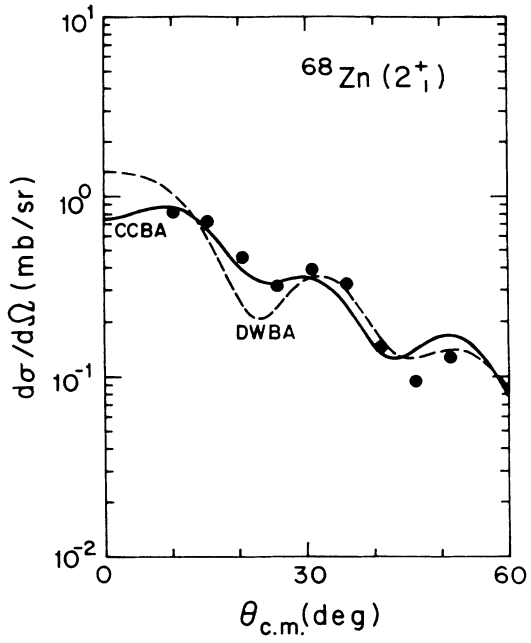

FIG. 10. Plot of the CCBA calculation coupling the three processes, UAO, OAU, and D with destructive coherent interference between the direct g.s.→g.s. component and the direct g.s.→2_1^+ component [i.e., sign combination (−, +)] and the angular distribution for the 1.078-MeV state in ^{68}Zn along with the DWBA results.

As a final remark here, we also considered CCBA calculations using the adopted values of β_2(^{70}Zn) and β_2(^{68}Zn) in the recent compilation of Raman *et al.*[19] These are given (in magnitude) for ^{70}Zn and ^{68}Zn as 0.228 and 0.205, respectively. We choose their signs to be negative and (as before) we consider all possible sign combinations. The results of these sets of calculations are not much different from the CCBA calculations just discussed in Figs. 8–10.

B. The 3_1^- state

As seen in Fig. 3, DWBA calculations with the optical-model parameters in Table I and the ($1g_{9/2}1f_{5/2}$) configuration are not capable of reproducing the angular distribution of the ^{70}Zn(p,t)^{68}Zn (2.749 MeV) data. Different choices for the two-neutron bound-state configuration only slightly affect the shape of the DWBA calculation. As in the ^{70}Zn(p,t)^{68}Zn (1.078 MeV) data above, we are forced to consider the possibility of fitting the data with a two-step direct CCBA calculation. We proceed in the same manner as above with the same notation (except that the 2_1^+ states are replaced by the 3_1^- states). The values of β_3 are taken from the compilation.[1,20] These were measured with (p,p') and are given as $|\beta_3|$=0.196 in ^{68}Zn and $|\beta_3|$=0.216 in ^{70}Zn. As before, we choose the signs of these to be negative. Figure 11 depicts the results for the UAO, OAU with their coherent sums and differences. One sees that the magnitude of the data is very nearly reproduced by considering only the UAO route of the CCBA calculation. The shape is also almost reproduced except for the forward angle point and the maximum at 35°. A look at Fig. 3 shows that the DWBA L=3 curve is maximum at the forward angle and then contains a second maximum at

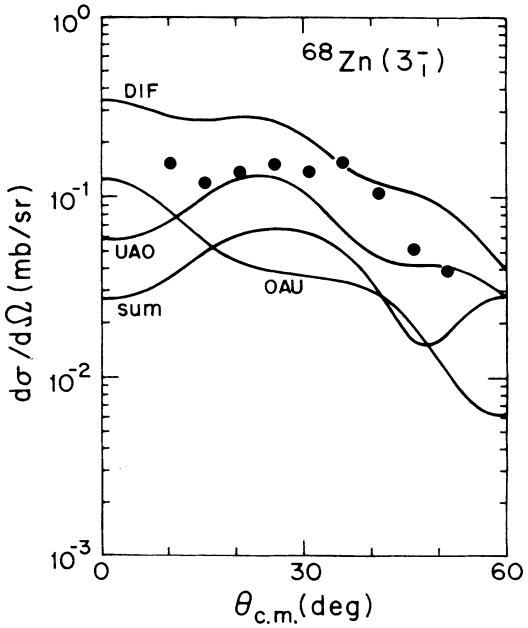

FIG. 11. Same as in Fig. 8 except using the 3_1^- states.

around 35°. Therefore, if one includes the direct ^{70}Zn(g.s.)$\rightarrow^{68}$Zn(3_1^-) route in the calculation, the fit to the data should improve. Figure 12 shows the result of including the direct ^{70}Zn(g.s.)$\rightarrow^{68}$Zn(3_1^-) route. For sign combinations (+,+) and (−,+), the *magnitude* of the data can be reproduced using appropriate values for the ^{70}Zn(g.s.)$\rightarrow^{68}$Zn(3_1^-) spectroscopic amplitude. On the other hand, for sign combinations (−,−) and (+,−), no amount of the ^{70}Zn(g.s.)$\rightarrow^{68}$Zn(3_1^-) route in the full UAO-OAU-*D* CCBA calculation will fit the magnitude of the data. By a coherent inclusion of the ^{70}Zn(g.s.)$\rightarrow^{68}$Zn(3_1^-) route, either destructively or constructively, the calculation always overestimates the magnitude of the data. The best fit then will occur when this strength is zero in which case we get back the |UAO-OAU| calculation (DIF) in Fig. 11. The *shape* of the ^{70}Zn(p,t)^{68}Zn(3_1^-) angular distribution is best reproduced using sign combination (+,+). In fact, the fit to the data (Fig. 13) is excellent, especially when compared to the original one-step DWBA calculation.

C. The 4_1^+ state

The first 4^+ state seen in ^{70}Zn(p,t) is at 2.418 MeV and is shown in Fig. 2 along with the DWBA calculation. The quality of the fit is good with the exclusion of the forward angle point at 10°. As discussed in Sec. IV this effect is present in all pure $L=4$ states seen in this work. In an attempt to improve the fit at the 10° point, we have performed CCBA calculations between the ground states, 2_1^+ states and 4_1^+ states in ^{68}Zn and ^{70}Zn. In principle, one can perform this calculation in the same manner as was done for the 2_1^+ and 3_1^- states in Secs. V A and B

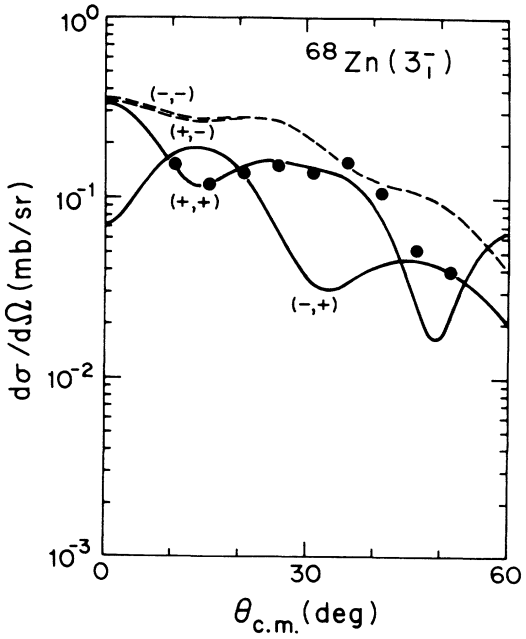

FIG. 12. Same as in Fig. 9 except using the 3_1^- states.

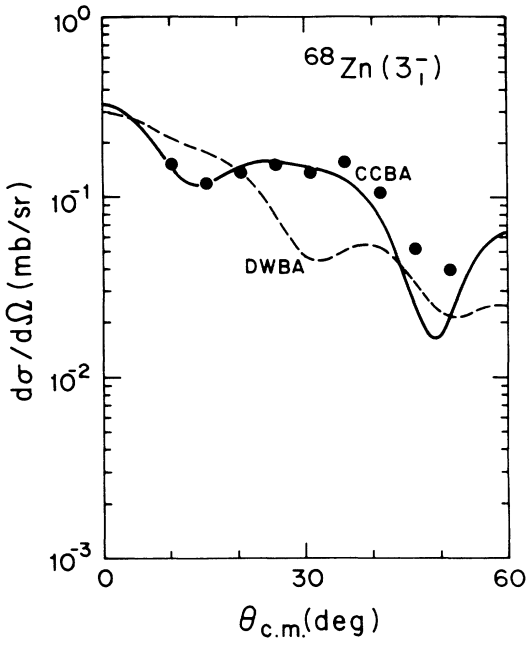

FIG. 13. Plot of the CCBA calculation coupling the three processes, UAO, OAU, and *D* with constructive coherent interference between the direct g.s.→g.s. component and the direct g.s.→3_1^- component [i.e., sign combination (+,+)] and the angular distribution for the 2.749-MeV state in ^{68}Zn along with the DWBA results.

where we would consider only the ground states and the 4_1^+ states and various couplings between them. However, the ^{68,70}Zn(g.s.)$\rightarrow^{68,70}$Zn(4_1^+) transitions have not been measured and so the experimental values of β_4 in ^{70}Zn and ^{68}Zn are not known. Therefore, we instead must consider the more complicated process which couples transitions between the ground states, 2_1^+ states and 4_1^+ states in ^{68,70}Zn. In principle, one could start this calculation with the simplier DWBA ^{70}Zn(g.s.)$\rightarrow^{68}$Zn(2_1^+) process as a foundation and consider ^{70}Zn(g.s.)$\rightarrow^{68}$Zn(2_1^+) $\rightarrow^{68}$Zn(4_1^+) denoted by OAU, and ^{70}Zn(g.s.)$\rightarrow^{70}$Zn(2_1^+) $\rightarrow^{68}$Zn(4_1^+) denoted by UAO with constructive and destructive interferences of each. The strength of the ^{70}Zn(g.s.)$\rightarrow^{68}$Zn(2_1^+) route [which is assumed equal in magnitude to the strength of the ^{70}Zn(2_1^+)$\rightarrow^{68}$Zn(4_1^+) route] is chosen so as to fit the normalized DWBA calculation. The remaining ^{70}Zn(g.s.)$\rightarrow^{70}$Zn(2_1^+) and ^{68}Zn(2_1^+)$\rightarrow^{68}$Zn(4_1^+) routes are given a strength represented by the β_2 value of −0.19 used in Sec. V A. The results of these calculations are shown in Fig. 14 and it is clear that the *magnitude* of the data is very nearly reproduced. In fact these calculations encourage one to perform the more detailed CCBA described below.

Based on the results of Sec. V A, we choose as a more precise foundation for the CCBA calculation the (−,+) CCBA calculation which reproduced the 2_1^+ state. We indicate schematically in Fig. 15 the various coupling routes in this calculation. These include inelastic *E*2 transitions (all having strength $\beta_2=-0.19$) between g.s.↔2_1^+ and between $2_1^+\leftrightarrow 4_1^+$ assuming that *both*

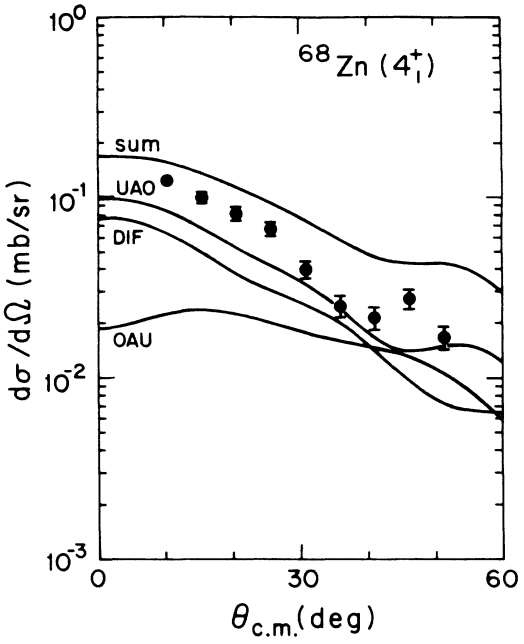

FIG. 14. Same as in Fig. 8 except using the ^{70}Zn(g.s.)$\rightarrow^{68}$Zn(2_1^+)$\rightarrow^{68}$Zn(4_1^+) as the OAU route and the ^{70}Zn(g.s.)$\rightarrow^{70}$Zn(2_1^+)$\rightarrow^{68}$Zn(4_1^+) as the UAO route.

directions are possible: the ^{70}Zn(g.s.)$\rightarrow^{68}$Zn(g.s.), ^{70}Zn(2_1^+)$\rightarrow^{68}$Zn(2_1^+), and ^{70}Zn(4_1^+)$\rightarrow^{68}$Zn(4_1^+) processes (labeled with strengths given by D_{00}, D_{22}, and D_{44}, respectively); the ^{70}Zn(g.s.)$\rightarrow^{68}$Zn(2_1^+) and ^{70}Zn(2_1^+) $\rightarrow^{68}$Zn(4_1^+) processes (labeled with strengths given by D_{02} and D_{24}, respectively); and the ^{70}Zn(g.s.)$\rightarrow^{68}$Zn(4_1^+) process labeled with a strength given by D_{04}. We note here that the strengths D_{00} and D_{02} will be slightly different from those used in Sec. V A because here we are allowing for $E2$ flux between the ground states and 2_1^+ states in *both* directions whereas the calculation in Sec. V A assumed only unidirectional $E2$ flux from the ground state to the 2^+ states. We determine the strength D_{00} (which we assume equal in magnitude to D_{22} and D_{44}) by fitting to the ^{70}Zn(p,t)^{68}Zn(g.s.) angular distribution in both shape and magnitude. We determine the strength D_{02} (which we assume equal in magnitude to D_{24}) by

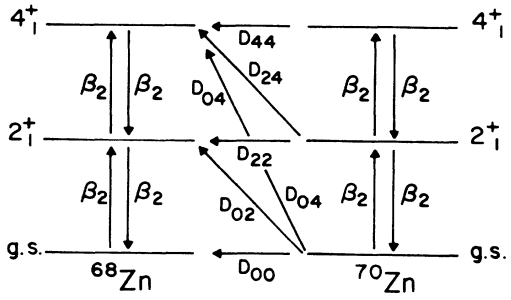

FIG. 15. Schematic representation of the coupled processes involved in the CCBA calculation of the ^{70}Zn(p,t)^{68}Zn(4_1^+) angular distribution.

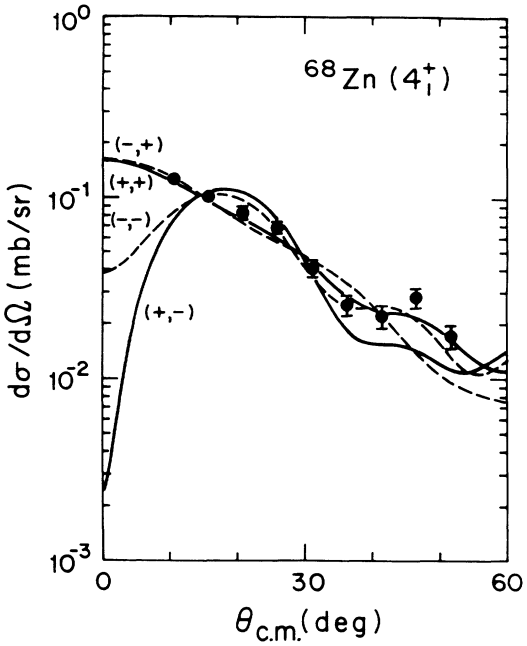

FIG. 16. Coupled-channels calculations for coupled combinations between the seven processes D_{00}, D_{22}, D_{44}, D_{02}, D_{24}, D_{04}, and β_2 along with the ^{70}Zn(p,t)^{68}Zn(4_1^+) angular distribution. In all four curves, the strength of the ^{70}Zn(g.s.)$\rightarrow^{68}$Zn(4_1^+) route (i.e., D_{04}) has been varied to give the best fit magnitude to the measured ^{70}Zn(p,t)^{68}Zn(4_1^+) cross section.

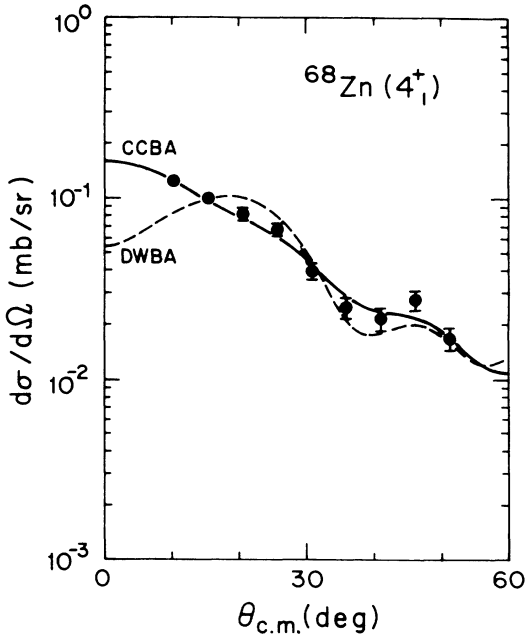

FIG. 17. Plot of the CCBA calculation coupling the seven processes D_{00}, D_{22}, D_{44}, D_{02}, D_{24}, D_{04}, and β_2 with constructive coherent interference between the g.s.$\rightarrow 4_1^+$ component D_{04}, and the $4_1^+\rightarrow 4_1^+$ component D_{44} [i.e., sign combination (+,+)], and the angular distribution for the 2.418-MeV state in ^{68}Zn along with the DWBA results.

fitting the ground-state and 2^+-state coupled processes to the ^{70}Zn$(p,t)^{68}$Zn(2_1^+) angular distribution in both shape and magnitude. The only unknown strength is D_{04} which we determine by fitting to the ^{70}Zn$(p,t)^{68}$Zn(4_1^+) angular distribution in both shape and magnitude. Since we are using the sign combinations (with slightly adjusted magnitudes to account for the g.s.$\leftrightarrow 2_1^+$ $E2$ flux in both directions) for D_{00}, D_{02}, and β_2 as determined by the best fit to the ^{68}Zn(2_1^+) state in Sec. V A, only the signs of D_{04} and D_{44} are ambiguous. This leads to four possible sign combinations in (D_{44},D_{04}) which we label as $(-,+)$, $(+,+)$, $(-,-)$, and $(+,-)$, respectively. The results of these CCBA calculations are shown in Fig. 16 and it is clear that one can fit the magnitude of the ^{70}Zn$(p,t)^{68}$Zn(4_1^+) angular distribution for any choice of sign in D_{44} and D_{04}. The shape of this angular distribution (especially at forward angles) is reproduced by either the $(-,+)$ or the $(+,+)$ combination with the latter being a little better at the larger angles. We show in Fig. 17 this best-fit CCBA calculation, the DWBA calculations and the 4_1^+ data.

VI. DISCUSSION OF LEVELS SEEN IN ^{66}Zn

There was enough ^{68}Zn present ($\approx$4.65%) in the ^{70}Zn target used that we were able to cleanly resolve the ground state and first 2^+ state in ^{66}Zn. These angular distributions are presented in Fig. 18 and have shapes which are fitted, respectively, by $L=0$ and $L=2$ curves. These results are consistent with the compilations. Note that for both levels, we get almost perfect agreement with the DWBA calculations using the optical-model parameters of Table I. There is a slight amount of filling in the first minimum of the angular distribution of the 2_1^+ level, but the forward-angle slope of the data is nicely reproduced in DWBA. It is interesting here that the 2_1^+ is fitted reasonably well by DWBA suggesting a direct one-step process unlike the results shown above for ^{70}Zn(p,t) and other (p,t) reactions leading to the 2_1^+ states in ^{74,76}Se (Ref. 12) and ^{38}Ar.[18]

VII. SUMMARY AND CONCLUSIONS

We have reported on 18 levels populated in the ^{70}Zn$(p,t)^{68}$Zn reaction at $E_p=35$ MeV. DWBA calculations can account for the shapes of the angular distributions for almost all levels except for that of the 2_1^+ state

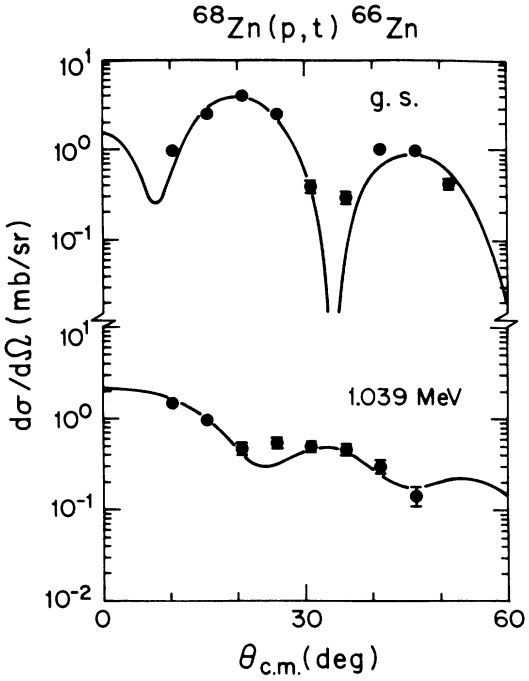

FIG. 18. Angular distributions and DWBA fits for ground state and 2_1^+ state seen in ^{66}Zn.

at 1.078 MeV, the 3_1^- state at 2.749 MeV, and forward-angle points of the 4^+ states at 2.418, 2.957, 3.275, 3.577, and 4.110 MeV. All other observed 2^+ angular distributions have shapes that are fitted quite well by only the ^{70}Zn(g.s.)$\rightarrow^{68}$Zn(2^+) route (i.e., DWBA). We have shown for the lowest, $J^\pi=2^+$ 3^-, and 4^+ states that a two-step direct process using the code CHUCK can account for both the magnitudes and shapes of the ^{70}Zn$(p,t)^{68}$Zn(J_1^π) angular distributions provided we allow for contributions from the ^{70}Zn(g.s.)$\rightarrow^{68}$Zn(J_1^π) route. We have also measured the $\sigma(0_2^+)/\sigma$(g.s.) ratio ($\approx$18%) to be used as input into a two-state model analysis[4] of zinc isotopes as was done for germanium.[3]

We are grateful to Mr. Laszlo Csihas for his careful preparation of the ^{70}Zn targets and we acknowledge financial support from the National Science Foundation.

*Present address: QUANTICS Inc., 993 Old Eagel School Rd., Wayne, PA 19087.
†Present address: Department of Physics, University of Richmond, Richmond, VA 23284.
‡Present address: Division of Physics, Argonne National Laboratory, Argonne, IL 60439.
§Present address: Department of Physics, University of Notre Dame, South Bend, IN 46556.
**Present address: Oak Ridge National Lab, Box X, Oak Ridge, TN 37830.

[1]F. Kearns, Nucl. Data Sheets **33**, 481 (1981).
[2]L. C. McIntyre, Phys. Rev. **152**, 1013 (1966).
[3]M. Carchidi, H. T. Fortune, G. S. F. Stephans, and L. C. Bland, Phys. Rev. C **30**, 1293 (1984).
[4]M. Carchidi and H. T. Fortune, Phys. Rev. C **37**, 556 (1988).
[5]R. T. Kouzes and D. Muller, Nucl. Phys. **A307**, 71 (1978).
[6]P. D. Kunz, Programs DWUCK4 and CHUCK4, University of Colorado (unpublished); extended version of J. R. Comfort

(unpublished).
[7]F. G. Perey, Phys. Rev. **131**, 745 (1963).
[8]R. A. Hardekopf, L. R. Veeser, and P. W. Keaten, Jr., Phys. Rev. Lett. **35**, 1623 (1975).
[9]J. F. Mateja *et al.*, Phys. Rev. C **17**, 2047 (1978).
[10]L. H. Rosier *et al.*, Nucl. Phys. **A453**, 389 (1986).
[11]F. R. Hudson and R. N. Glover, Nucl. Phys. **A189**, 264 (1972).
[12]M. Borsaru *et al.*, Nucl. Phys. **A284**, 379 (1977).
[13]A. S. Litvinenko *et al.*, Yad. Fiz. **18**, 250 (1973) [Sov. J. Nucl. Phys. **18**, 128 (1974)].
[14]R. Neuhausen, J. W. Lightbody, Jr., S. P. Fivozinsky, and S. Penner, Nucl. Phys. **A263**, 249 (1976).
[15]R. Neuhausen, Nucl. Phys. **A282**, 125 (1977).
[16]R. A. Hinrichs and D. M. Patterson, Phys. Rev. C **10**, 1381 (1974).
[17]E. Fabriai *et al.*, Phys. Rev. C **21**, 844 (1980).
[18]K. Miura, Y. Hiratate, T. Shoji, and T. Suehiro, Nucl. Phys. **A334**, 389 (1980).
[19]S. Raman *et al.*, At. Data Nucl. Data Tables **36**, 11 (1987).
[20]M. R. Bhat, Nucl. Data Sheets **51**, 95 (1987), and references therein.